

Straightening of curved pattern of collagen fibers under load controls aortic valve shape

Peter E. Hammer^{a*}, Christina A. Pacak^b, Robert D. Howe^c, Pedro J. del Nido^a

^a*Department of Cardiac Surgery, Boston Children's Hospital, Boston, MA, USA*

^b*Department of Anesthesia, Boston Children's Hospital, Boston, MA, USA*

^c*Harvard School of Engineering and Applied Sciences, Cambridge, MA, USA*

Keywords: Finite element model, Aortic valve, Collagen pattern

ABSTRACT

The network of collagen fibers in the aortic valve leaflet is believed to play an important role in the strength and durability of the valve. However, in addition to its stress-bearing role, such a fiber network has the potential to produce functionally important shape changes in the closed valve under pressure load. We measured the average pattern of the collagen network in porcine aortic valve leaflets after staining for collagen. We then used finite element simulation to explore how this collagen pattern influences the shape of the closed valve. We observed a curved or bent pattern, with collagen fibers angled downward from the commissures toward the center of the leaflet to form a pattern that is concave toward the leaflet free edge. Simulations showed that these curved fiber trajectories straighten under pressure load, leading to functionally important changes in closed valve shape. Relative to a pattern of straight collagen fibers running parallel to the leaflet free edge, the concave pattern of curved fibers produces a closed valve with a 40% increase in central leaflet coaptation height and with decreased leaflet billow, resulting in a more physiological closed valve shape. Furthermore, simulations show that these changes in loaded leaflet shape reflect changes in leaflet curvature due to modulation of in-plane membrane stress resulting from straightening of the curved fibers. This effect appears to play an important role in normal valve function and may have important implications for the design of prosthetic and tissue engineered replacement valves.

* Address correspondence to: Peter E. Hammer, Department of Cardiac Surgery, Boston Children's Hospital, 300 Longwood Ave., Boston, MA, USA, (617) 919-2317. E-mail address: peter.hammer@childrens.harvard.edu.

1. Introduction

The aortic valve acts as a check valve to ensure one-way blood flow from the left ventricle into the aorta. The normal valve has three leaflets, controlled by pressure gradients, which present negligible outflow resistance when open during cardiac ejection and close without leak during ventricular filling to maintain diastolic pressure in the aorta and systemic circulation. A healthy valve opens and closes competently over billions of cycles and a wide range of heart rates and blood pressures. This durability is attributed to the heterogeneous, layered arrangement of structural proteins and proteoglycans in the leaflets, with a hierarchical network of collagen fibers believed to bear most of the stress during loading (Sacks et al., 2007). The biomechanics of the aortic valve has been the subject of rigorous study, motivated by the hope that a better understanding of normal valve function will increase understanding of valve disease progression and lead to improved prosthetic valves and to more reliable methods for valve surgical repair.

Computational models have been used to study the relationship between aortic valve structure and function (DeHart et al., 2004; Grande et al., 2000; Koch et al., 2012; Labrosse et al., 2010; Ranga et al., 2004; Weinberg et al., 2007). Such models are valuable both to codify existing knowledge of valve structure and tissue properties and to enable the study of individual effects of different features and properties on valve function. We have used computational modeling to study aortic valve surgical repair (Hammer et al., 2012a), focusing on structural finite element models that can simulate the closed valve during diastole, when the repaired valve subject to its maximum structural loads and most likely to leak. Our initial model incorporated a published, geometrical description of leaflet shape, an experimentally-derived nonlinear orthotropic constitutive law for leaflet tissue, and a principal material direction - corresponding to the collagen fiber network - running in straight lines across each leaflet parallel to the free edge. Simulations predicted a loaded valve in which the leaflets closed completely but without the overlap, termed coaptation, typical of a normal aortic valve. Furthermore, the simulation exhibited greater billow of the closed leaflets than a normal, healthy valve. We hypothesized, based on preliminary observations of isolated aortic valve leaflets, that the principal fiber direction in the normal aortic valve leaflet in its unstrained configuration is not strictly uniform across the leaflet but rather forms a series of curved or bent trajectories and that this curved fiber pattern has an important effect on the shape of the closed valve under pressure load (Hammer, 2011a).

In this study, we measure the orientation of macroscopically visible collagen bundles in the unstrained aortic valve leaflets of seven porcine hearts, and we explore the effect of the pattern of collagen fiber bundles on the shape of the closed aortic valve under load. We test the effect of collagen bundle orientation on the loaded valve using a structural finite element model. Average leaflet shape and collagen bundle orientation in the model are measured from the porcine valves. We compare the effect of varying the fiber pattern on leaflet coaptation and closed valve shape, examining the role of the patterned fibers in modulating leaflet stress and, consequently, curvature of the loaded leaflets.

2. Methods

2.1. Determining pattern of collagen network

Aortic valve leaflets were excised along their lines of attachment to the aortic root from 18 fresh porcine hearts. For all 18 valves, the planar outlines of each of the three leaflets were measured in the unstrained configuration by placing the leaflets in a Petri dish on a thin layer of phosphate-buffered saline (PBS) and photographing them on a white light box using a 9 megapixel digital SLR camera. To better visualize the network of collagen bundles, which was typically not visible throughout much of the thick central region of the transilluminated leaflets, we stained the leaflets of seven of the valves for collagen. We analyzed

only this subsample (seven) of the valves for collagen due to the laboriousness of the process. The leaflets were submerged in Sircol dye reagent (Sircol Collagen Assay, Biocolor, UK) for 30 minutes, rinsed in PBS, then placed in 0.05% trypsin for 48 hours at 37°C to remove the surface layer of endothelial cells. Leaflets were then rinsed in PBS and placed in 0.5 M sodium acetate for 5 days to remove soluble proteins including proteoglycans. The leaflets were then rinsed, and any remaining unstained tissue was excised. Each leaflet was again photographed on the light box to image the collagen structure (dyed red).

The planar outline of each leaflet was digitized by manually tracing on the digital image. The average leaflet outline for each left coronary (LC), right coronary (RC), and non-coronary (NC) leaflet was computed by aligning and normalizing each tracing to the two termini of the free edge, resampling each outline at 300 equally-spaced points, then averaging the locations of those points across all 18 valves.

The orientation of collagen bundles in the stained leaflet images was quantified by computing the 2-d structure tensor at all image pixels (Kothe, 2003). For an image intensity I of two variables, x and y , the 2-element gradient vector at each pixel is

$$\nabla I = \begin{pmatrix} \frac{\partial I}{\partial x} & \frac{\partial I}{\partial y} \end{pmatrix}, \quad (1)$$

and the 2 x 2 gradient tensor is computed as

$$S_0 = (\nabla I)^T (\nabla I). \quad (2)$$

Spatially weighting this tensor function results in the 2 x 2 structure tensor

$$S_w(p) = \int_r w(r) S_0(p-r) dr, \quad (3)$$

where p is point (x,y) in the image, w is a weighting function, and r is a weighting neighborhood around p . This quantity was computed for all pixels lying within a leaflet boundary. A pixel was determined to lie on or near oriented structure (i.e., a bundle of collagen fibers) if the ratio of the maximum to the minimum eigenvalue of the structure tensor exceeds 10:1. The orientation of the tissue structure at that pixel was computed as the angle, relative to the line through the leaflet free edge termini, of the eigenvector associated with the smaller eigenvalue. Direction vectors were flipped as necessary to result in orientations, specified as angles between -90° and 90°. To compare collagen orientation data across all valves, each leaflet image was divided into a 4 x 8 grid of subregions, and the orientation for a given subregion for a given leaflet was computed as the mean orientation of all pixels associated with oriented structure, as defined above, for that subregion and leaflet. Orientation within each subregion was computed for all seven leaflets of each type (LC, NC, and RC). To assess the variability in orientation across the seven valves, we analyzed the orientation data using circular statistics (Fisher 1993; Zar 1999). A Rayleigh test was used to test the null hypothesis that the samples of orientation in each subregion across the seven valves are drawn from a uniform circular (i.e., random) distribution, with the alternative hypothesis that they are drawn from a unimodal distribution – specifically from a circular normal (i.e., Von Mises) distribution (Fisher 1993).

2.2. Computational valve model to study effect of fiber pattern

A structural finite element model of the aortic valve was constructed based on the computed average shapes of the LC, NC and RC leaflets and was used to compute the geometry of the closed, loaded valve as a function of the pattern of collagen orientation. First, an unstructured mesh of approximately 600 triangles is generated within the three leaflet outlines. Then, based on the published observation that the aortic valve leaflet attachment lies on a cylinder (Labrosse et al., 2006; Swanson et al., 1974), the planar leaflet meshes are connected at the free edge termini and wrapped into a cylinder. The loaded valve is simulated by first computing the positions of the boundary nodes (i.e., where the leaflets attach to the aortic root) at diastole then applying diastolic pressure to close and load the leaflets. The aortic root, which contains the mesh boundary points, is modeled as a linearly elastic cylindrical tube using published values of Young's modulus and thickness (Grande et al., 1998), and the diameter of the root in diastole is determined using a force balance between a transluminal pressure of 80 mmHg and the wall stress in the cylinder. Then a pressure of 80 mmHg is applied to the aortic surface of the leaflets to simulate leaflet closure and loading. The leaflets are modeled using three node membrane elements with an experimentally-derived orthotropic hyperelastic constitutive equation (Hammer et al., 2011b). The principal material direction, corresponding to the local angle of collagen fiber bundles, was assigned to mesh elements to reflect the overall fiber orientation pattern observed in the leaflet images using the methods in section 2.1. We simulate the equations of motion, including contact handling, and solve for the final deformed state of the valve using a large deformation finite element model formulated for membrane elements and incorporating semi-implicit numerical integration and error-based time step control. Simulation and post processing software were written in the Matlab programming language (Mathworks, Inc., Natick, MA, USA). For further details of the aortic valve computational model, see (Hammer et al., 2012a). The structural finite element model was validated in our previous work using simulated biaxial loading of square patches of leaflet tissue (Hammer et al., 2011b) and using ex vivo experiments of pressurized isolated aortic valves (Hammer et al., 2012a).

3. Results

Images of the stained leaflets show a pattern of macroscopically visible collagen fiber bundles originating from the commissures and angled downward toward the leaflet midline. It is also possible to observe that as the large collagen bundles separate, many of the branches form continuous arcs, concave toward the leaflet free edge, across the leaflet (Fig. 1).

Analysis of collagen fiber angle across all seven valves shows that for each of the three leaflet types, collagen fibers tend to be oriented downward from the commissures toward the leaflet midline (Fig. 2B, E, and H), with the highest prevalence of oriented structure and largest absolute angles (typically 20 to 30°) occurring in the upper quadrants of the leaflets. In the bottom row of leaflet subregions, highly oriented structure is much less prevalent and, when present, is typically shown by the Rayleigh test to correspond to randomly oriented structure.

In order to study the isolated effect of the collagen pattern that we observe on aortic valve function, we model the fiber pattern using a single parameter: the absolute collagen angle, ϕ , with respect to the line through the termini of the leaflet free edge. For mesh elements comprising the leaflet free edge, the principal material direction is defined as the local direction of the free edge, reflecting the collagen bundle typically observed to bound the free edge. For mesh elements lying in the top 75% of the leaflet, the principal direction is defined by an angle of negative ϕ in the left half of the leaflet and positive ϕ in the right half of the leaflet, while for mesh elements in the lower 25% of the leaflet, the local fiber angle is taken as zero degrees (Fig. 3). The loaded state of the valve was simulated for 9 different meshes

corresponding to collagen fiber angle, ϕ , of 0 to 40° in increments of 5° (Fig. 4A-B). Simulation results of the closed state of the valve under load showed that the angled pattern of the principal material direction produces a decrease in curvature (flattening) of the lower central portion of the leaflets and an increase in curvature in the upper central portion at the base of the coaptation region, resulting in increased central coaptation height as seen in cross sections at the leaflet midline (Fig. 5).

The shape of the leaflet region involved in coaptation is visualized by demarcating it on the undeformed leaflet outline (Fig. 4C-D). The height of coaptation in the center of the closed valve can be measured from the simulated closed valves, and plotting central coaptation height as a function of fiber angle, ϕ , shows that mean central coaptation height increases by 40% as ϕ increases over the range of simulated angles (Fig. 6). Principal stresses in the leaflets are visualized by superimposing color maps of stress (second Piola-Kirchhoff stress) on the undeformed leaflets (Figs. 4E-F and 4G-H). Plotting the second principal stress computed along the leaflet midline shows that as fiber angle is increased, stress is increased in the lower central portion of the leaflets and decreased in the upper central portion of the leaflets at the base of the coaptation region (Fig. 7).

4. Discussion

One finding of this study is that the predominant pattern of collagen fibers in aortic valve leaflets in the unstrained state is nonuniform, running in a curved or v-shaped pattern from the commissures downward toward the leaflet midline. Descriptive accounts of aortic valve leaflet structure have often reported the collagen pattern as running parallel to the leaflet free edge (Sauren et al., 1980; Christie, 1992; Misfield et al., 2007), however quantitative analysis using small angle light scattering has shown a map of collagen fiber direction at the microscopic level that is similar to the pattern measured using our method (Sacks et al., 1998). A more recent study of aortic valve collagen mesostructure using elliptically polarized light reported a similar pattern (Doehring et al. 2005). In fact, computational modeling has been used to show that the pattern that we have observed can develop as a result of collagen remodeling, with fibers aligning with principal strain directions within the leaflets (Driessen et al., 2003).

The second finding of this study is that simulations show that the observed pattern of collagen in the leaflets (i.e., concave toward the free edge) has a strong effect on the shape of the closed valve under load. In the normal valve, the three leaflets come together to form a nearly flat surface perpendicular to the axis of the aorta, and the leaflets exhibit a central coaptation (overlap) of 3-5 mm in height. Simulations that incorporate a straight pattern of fibers parallel to the leaflet free edge produce a closed valve with considerable billow toward the left ventricle and a central coaptation height of approximately 2 mm. Incorporating the observed, curved collagen pattern reduces the billow and increases central coaptation height to normal levels. Surgeons have noted that central coaptation is critical for normal valve function, and successful surgical repair of the valve is dependent upon a large central coaptation (Augoustides et al., 2010).

An important advantage to using a computational model to study the effect of a curved principal direction in aortic valve leaflets is the ability to understand the mechanism by which the curved collagen fiber pattern produces the advantageous shape changes observed in simulation. Analysis of leaflet stresses and of the shape of the simulated closed leaflets under load shows that as the curved collagen fiber trajectories straighten during pressure loading of the leaflet, the tensile stress in the radial direction (i.e., the second principal direction) is increased in the vicinity of the intersection of the leaflet midline with the aortic root. This fiber straightening also causes the radial tensile stress to decrease along the leaflet midline near the free edge. The product of membrane tensile stress and curvature is constant for a given transmembrane pressure according to Laplace's Law (Fung, 1981), so the regions of elevated tensile stress

(i.e., near the attachment of the leaflet) exhibit decreased curvature while regions of decreased tensile stress (i.e., the base of the coaptation region) exhibit increased curvature. In the loaded valve, these changes correspond to flattening of the leaflet belly and to displacing leaflet tissue tangentially toward the valve center producing greater central leaflet coaptation.

Other groups have studied the effect of patterned reinforcement fibers in polymer valves (Cacciola et al., 2000; Liu et al., 2007). These studies, however, only reported the effect on leaflet stresses, not shape, of the loaded valve. Interestingly, the results of Liu et al. showed that the optimal fiber pattern with regard to leaflet stress for a single-ply fiber-reinforced leaflet has the fibers oriented *upward* from the commissures toward the leaflet free edge. However, this pattern would result in tangential displacement of leaflet tissue away from the valve center during loading, reducing or eliminating central coaptation. A recent study (Fan et al., 2013) reproduced our preliminary result modeling the effect of a curved principal direction on the shape of the loaded leaflet (Hammer, 2011a), adjusting their material properties to simulate an elastomeric pulmonary valve scaffold. This is the first study to report the relationship between the curved collagen pattern in the normal aortic valve leaflet and the shape and coaptation changes of the leaflets of the closed valve under load.

One limitation of this study is the use of pig instead of human aortic valves, although the close similarity between porcine and human aortic valves has been reported, and the few normal human aortic valve leaflets that we have examined have similar gross collagen architecture to that of the porcine valves. Our computational model, while based on experimentally measured leaflet shapes and material law, still relies on the simplifying assumption that the orthotropic constitutive law is constant throughout each leaflet. We also make the assumption of constant leaflet thickness despite clear differences in thickness in different leaflet regions. This may be reasonable, however, for computing leaflet stress because the collagen rich layer that bears most of the stress is not noticeably thicker in the leaflet regions with increased thickness. Finally, when measuring the leaflet outlines in the unstrained configuration, we neglect the residual stress present in the leaflets. In fact, this residual stress was manifest as a small increase in leaflet height after dissolving and dissecting away the unstained tissue. However, our leaflet constitutive equation was based on biaxial testing of intact leaflet patches and thus includes effects of residual stress. Furthermore, we did not observe any consistent change in the pattern of the stained collagen fibers after the other leaflet tissues were dissolved and dissected away.

The effect of the curved collagen pattern could have important implications for the design of bioprosthetic replacement valves. By incorporating reinforcement fibers that mimic the ability of the native valve to flatten near the base of the leaflets and increase central coaptation height, it should be possible to design a valve with decreased leaflet height and, consequently, lower outflow resistance. There is also evidence to suggest that the curved fibers help to dampen transient stresses in the leaflets immediately following closure (Hammer et al., 2012b). The effect of the curved collagen pattern might also be important for scaffold design for tissue engineered valves, where a more natural pattern of cyclic stress in the leaflets could produce a milieu more conducive to normal signaling and gene expression in resident valve interstitial and endothelial cells.

Conflict of interest statement

We have no financial or personal conflicts of interest to disclose.

Acknowledgements

This work was supported by grant R01 HL110997 from the National Institutes of Health.

References

- Augoustides, J.G., Szeto, W.Y., Bavaria, J.E., 2010. Advances in aortic valve repair: focus on functional approach, clinical outcomes, and central role of echocardiography. *J. Cardiothorac. Vasc. Anesth.* 24, 1016-1020.
- Cacciola, G., Peters, G.W.M., Schreurs, P.J.G., 2000. A three-dimensional mechanical analysis of a stentless fibre-reinforced aortic valve prosthesis. *J. Biomech.* 33, 521-530.
- Christie, G.W., 1992. Anatomy of aortic heart valve leaflets: the influence of glutaraldehyde fixation on function. *Eur. J. Cardiothorac. Surg.* 6, S25-S33.
- De Hart, J., Peters, G.W.M., Schreurs, P.J.G., Baaijens, F.P.T., 2004. Collagen fibers reduce stresses and stabilize motion of aortic valve leaflets during systole. *J. Biomech.* 37, 303-311.
- Doehring, T.C., Kahelin, M., Vesely, I., 2005. Mesostructures of the aortic valve. *J. Heart Valve Dis.* 14(5), 679-686.
- Driessen, N.J.B., Boerboom, F.A., Huyghe, J.M., Bouten, C.V.C., Baaijens, F.P.T., 2003. Computational analyses of mechanically induced collagen fiber remodeling in the aortic heart valve. *J. Biomech. Eng.* 125, 549-557.
- Fan, R., Bayoumi, A.S., Chen, P., Hobson, C.M., Wagner, W.R., Mayer, J.E., Sacks, M.S., 2013. Optimal elastomeric scaffold leaflet shape for pulmonary heart valve leaflet replacement. *J. Biomech.* 46, 662-669.
- Fisher, N.I., 1993. *Statistical analysis of circular data.* Cambridge University Press, Cambridge, UK.
- Fung, Y.C., 1981. *Biomechanics: mechanical properties of living tissues.* Springer-Verlag, NY, pp. 17-18.
- Grande, K.J., Cochran, R.P., Reinhall, P.G., Kunzelman, K.S., 1998. Stress variations in the human aortic root and valve: the role of anatomic asymmetry. *Annals of Biomedical Engineering* 26(4), 534-545.
- Grande, K.J., Cochran, R. P., Reinhall, P. G., Kunzelman, K. S., 2000. Mechanisms of aortic valve incompetence: finite element modeling of aortic root dilatation. *The Annals of Thoracic Surgery* 6, 1851-1857.
- Hammer P.E., 2011a. *Simulating heart valve mechanical behavior for planning surgical repair.* PhD. thesis, Tufts University, Medford, MA, USA.
- Hammer, P. E., Sacks, M. S., del Nido, P. J., Howe, R. D., 2011b. Mass-spring model for simulation of heart valve tissue mechanical response. *Annals of Biomedical Engineering* 39, 1668-1679.
- Hammer, P.E., Chen, P.C., del Nido, P.J., Howe, R.D., 2012a. Computational model of aortic valve surgical repair using grafted pericardium. *J. Biomech.* 45, 1199-1204.
- Hammer, P.E., Howe, R.D., del Nido, P.J., 2012b. Lower transient stresses in an aortic valve leaflet with oblique reinforcement fibers: a finite element study. *Proc. ASME Summer Bioeng. Conf.*, June 20-23, Fajardo, PR.
- Koch, T.M., Reddy, B.D., Zilla, P., Franz, T., 2012. Aortic valve leaflet mechanical properties facilitate diastolic valve function. *Comput. Methods Biomech. Biomed. Engin.*, 13, 225-234.
- Kothe, U., 2003. Edge and junction detection with an improved structure tensor. In: Michaelis, B., Krell, G. (Eds.), *Lecture Notes in Computer Science.* Springer, Berlin, vol. 2781, pp. 25-32.
- Labrosse, M.R., Beller, C.J., Robicsek, F., Thubrikar, M.J., 2006. Geometric modeling of functional trileaflet aortic valves: development and clinical applications. *Journal of Biomechanics* 39(14), 2665-2672.

- Labrosse, M. R., Lobo, K., Beller, C. J., 2010. Structural analysis of the natural aortic valve in dynamics: from unpressurized to physiologically loaded. *Journal of Biomechanics* 43(10), 1916-1922.
- Liu, Y., Kasyanov, V., Schoepfoerster, R.T., 2007. Effect of fiber orientation on the stress distribution within a leaflet of a polymer composite heart valve in the closed position. *J. Biomech.* 40, 1099-1106.
- Misfield, M., Sievers, H.-H., 2007. Heart valve macro- and microstructure. *Phil. Trans. R. Soc. B* 362, 1421-1436.
- Ranga, A., Mongrain, R., Mendes Galaz, R., Biadillah, Y., Cartier, R., 2004. Large-displacement 3D structural analysis of an aortic valve model with nonlinear material properties. *J. Med. Eng. Technol.* 28, 95-103.
- Sacks, M.S., Smith, D.B., Heister, E.D., 1998. The aortic valve microstructure: effects of transvalvular pressure. *J. Biomed. Mater. Res.* 41, 131-141.
- Sacks, M.S., Yoganathan, A.P., 2007. Heart valve function: a biomechanical perspective. *Philos. Trans. R. Soc. Lond. B. Biol. Sci.* 362, 1369-1391.
- Sauren, A.A.H.J., Kuijpers, W., van Steenhoven, A.A., Veldpaus, F.E., 1980. Aortic valve histology and its relation with mechanics—Preliminary report. *J. Biomech.* 13, 97-104.
- Swanson, M., Clark, R.E., 1974. Dimensions and geometric relationships of the human aortic valve as a function of pressure. *Circulation Research* 35(6), 871-882.
- Weinberg, E.J., Mofrad, M.R.K., 2007. Transient, three-dimensional, multiscale simulations of the human aortic valve. *Cardiovasc Eng.* 7, 140-155.
- Zar J.H., 1999. *Biostatistical analysis*. Prentiss-Hall Inc., Upper Saddle River, NJ, pp. 592 – 660.



Fig. 1. Right coronary (RC) leaflet of porcine aortic valve photographed on a light table lying on a thin layer of PBS. Leaflet was stained (red) for collagen.

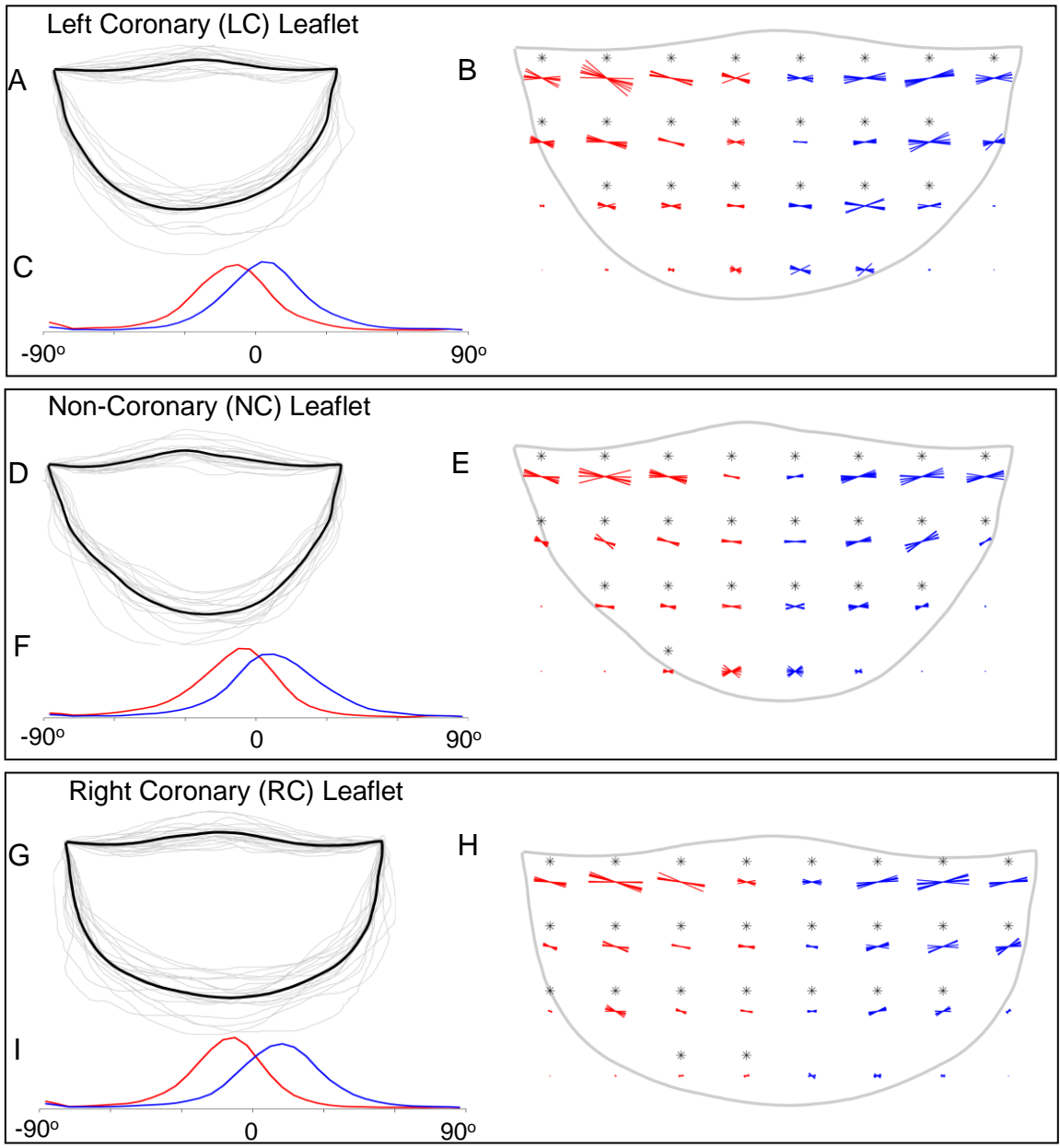


Fig. 2. Outlines for the left (A), non- (D), and right (G) coronary leaflets, with mean outline shown in black and individual outlines shown in gray. In B, E, and H, the leaflet is divided into 4 x 8 subregions, and the mean fiber orientation within each subregion for each of the seven stained valves is shown as a red/blue line segment for the left/right half of the leaflet, for the LC, NC, and RC leaflets, respectively. Segment length is proportional to the number of image pixels in each subregion where oriented structure was detected (see text), and an asterisk marks subregions where the null hypothesis of random orientation across the seven stained valves can be rejected ($P < 0.001$). Plots of the relative frequency of angles of oriented structure in the left (red) versus right (blue) sides of the leaflet midline are shown in C, F, and I for the LC, NC, and RC leaflets, respectively.

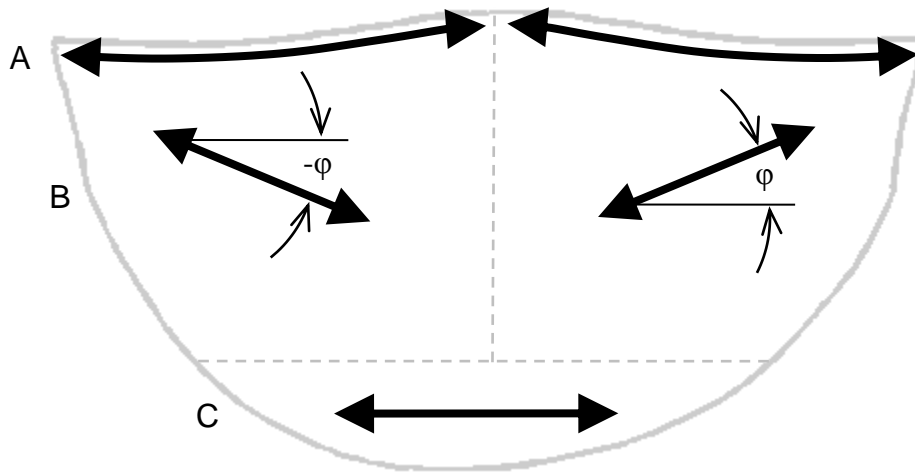
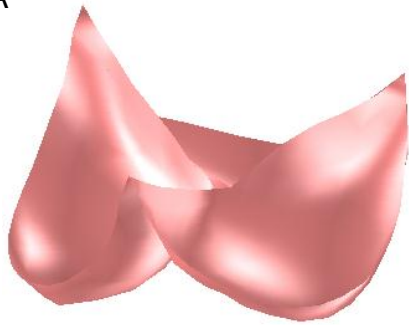


Fig. 3. For computational modeling of the leaflet tissue, the principal material direction was approximated as (A) the local direction of the leaflet free edge for mesh elements lying on the free edge, (B) at angle $-\phi$ ($+\phi$) for elements lying on the left (right) half of the upper 75% of the leaflet, and (C) in the horizontal direction (i.e., parallel to the line connecting the termini of the free edge) for elements lying in the lower 25% of the leaflet.

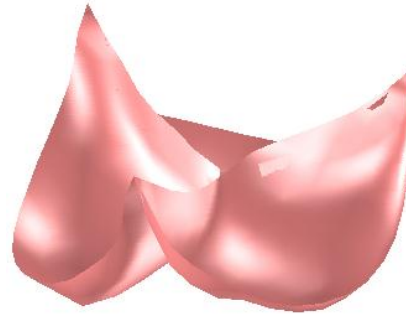
Principal Material Direction, $\varphi = 0^\circ$

Principal Material Direction, $\varphi = 30^\circ$

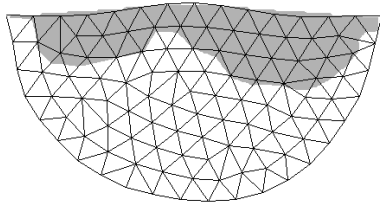
A



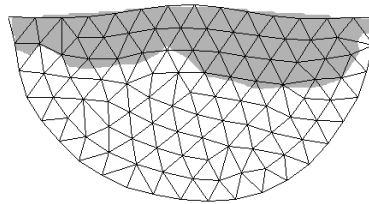
B



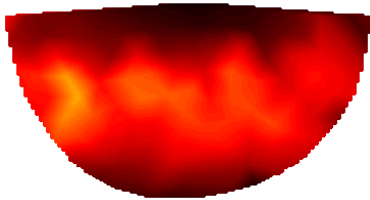
C



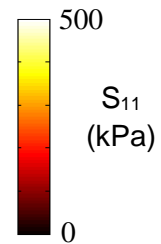
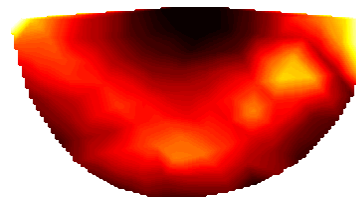
D



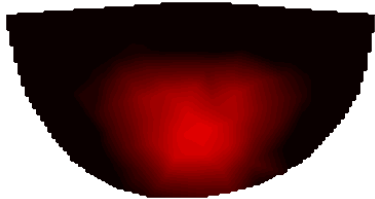
E



F



G



H

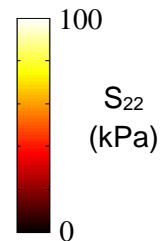
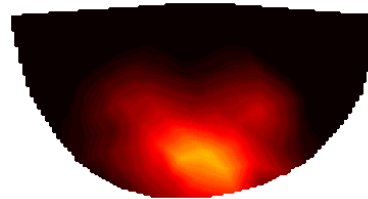


Fig. 4. (A&B): Simulated closed valve at 80 mmHg transvalvular pressure for $\varphi = 0^\circ$ and 30° , respectively. (C&D): Gray indicates portion of leaflet involved in coaptation for $\varphi = 0^\circ$ and 30° , respectively. (E&F): First principal stress (direction of collagen) for $\varphi = 0^\circ$ and 30° , respectively. (G&H): Second principal stress (direction perpendicular to collagen) for $\varphi = 0^\circ$ and 30° , respectively.

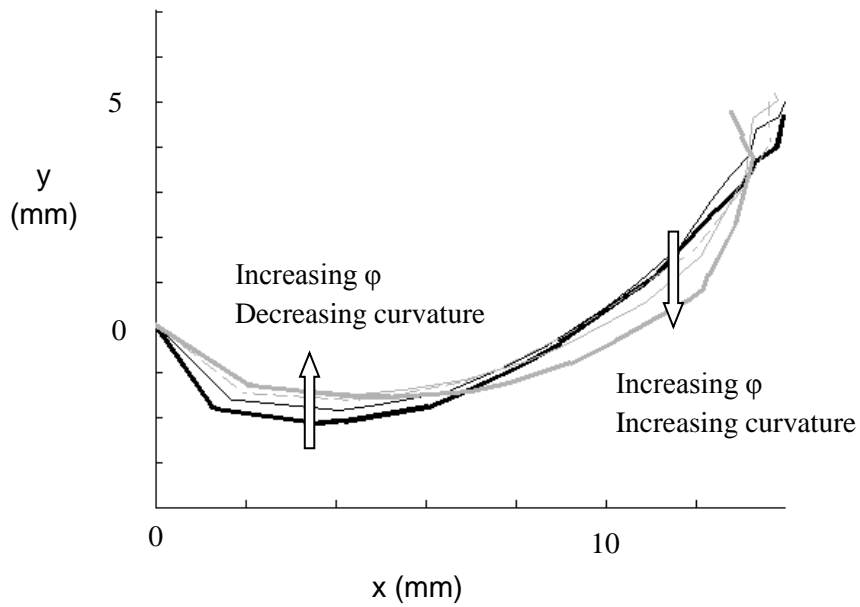


Fig. 5. Intersection of cut-plane with midline of left coronary leaflet of simulated closed valve for principal material angle, ϕ , of 0° (thick black), 10° (thin black), 20° (dashed gray), 30° (thin gray), and 40° (thick gray) curves.

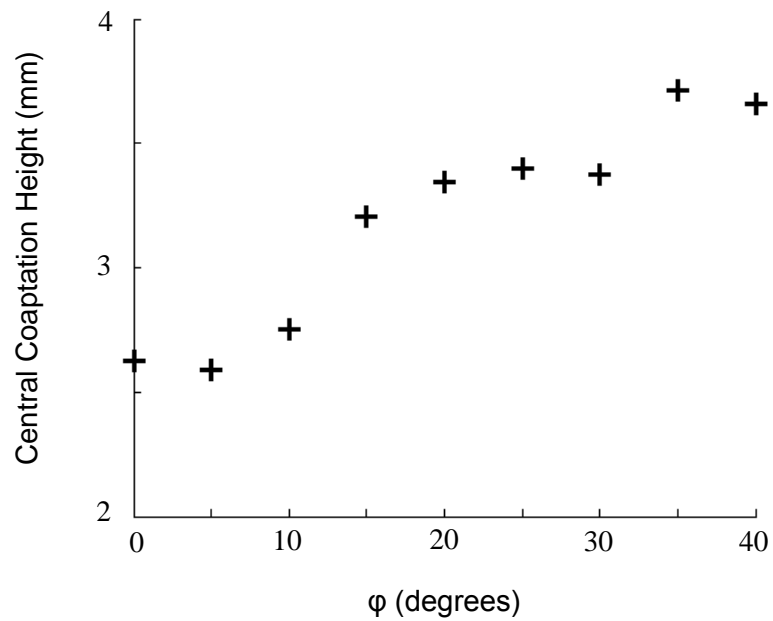


Fig. 6. Central coaptation height of simulated closed valve vs. the principal material direction angle, ϕ .

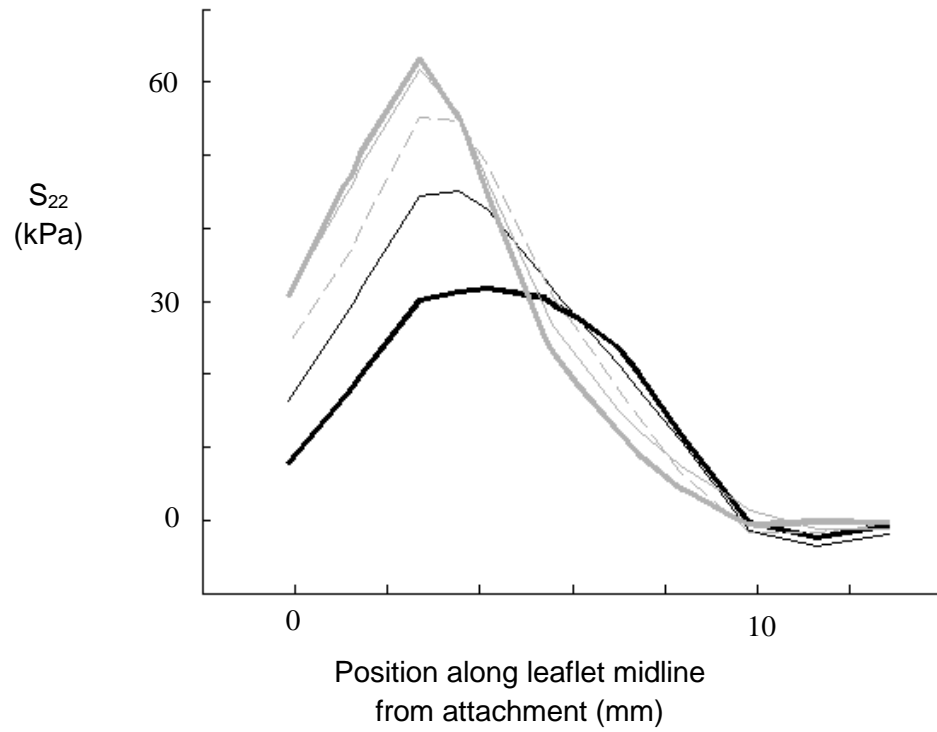


Fig. 7. Radial component of tensile stress (S_{22}) along leaflet midline for left coronary leaflet for angle $\phi = 0^\circ$ (thick black), 10° (thin black), 20° (dashed gray), 30° (thin gray), and 40° (thick gray) curves.